

The chondrocrania of North American *Rana* larvae (Anura: Ranidae): a morphological comparison

Peter M. Larson

Department of Biology, Saint Anselm College, Manchester, New Hampshire 03102, USA

Keywords:

chondrocranium, morphology, *Rana*, Ranidae, tadpole

Accepted for publication:

24 October 2007

Abstract

Larson, P.M. 2008. The chondrocrania of North American *Rana* larvae (Anura: Ranidae): a morphological comparison. — *Acta Zoologica* (Stockholm) 89: 279–288

A detailed morphological description of the chondrocranium is provided for the larvae of six species of North American *Rana*. Results indicated that although qualitative variation in chondrocranial morphology was limited among the larval *Rana* examined here, *R. sylvatica* is clearly distinguishable from other species based on the presence of a shorter articular process of the palatoquadrate, a wider muscular process of the palatoquadrate, and a more posterior position of attachment of the larval otic process to the palatoquadrate. These conditions are similar to those found in the Eurasian *R. temporaria*. *Rana clamitans* and *R. catesbeiana* are distinguished by a considerably narrower palatoquadrate in the region posterior to the anterior quadratocranial commissure, a more anterior position of attachment of the larval otic process to the palatoquadrate, and the presence of a lateral trabecular process in some specimens. These characters may represent larval synapomorphies for the traditional *R. catesbeiana* group (= *Aquarana*).

Peter M. Larson, Department of Biology, Saint Anselm College, Manchester, New Hampshire 03102, USA. E-mail: plarson@anselm.edu

Introduction

Frogs of the large, traditional genus *Rana* are among the most familiar and extensively studied of any group of anurans (Hillis 1988; Hillis and Wilcox 2005). Although hypotheses of phylogenetic relationships among species of New World *Rana* have been debated (Chantell 1970; Wallace *et al.* 1973; Case 1978; Farris *et al.* 1979, 1982; Post and Uzzell 1981; Hillis and Davis 1986; Uzzell and Post 1986; Hillis and de Sá 1988), recent molecular phylogenetic analyses have clarified these relationships considerably (Hillis and Wilcox 2005; Frost *et al.* 2006). Despite there being reasonable agreement among systematists regarding most details of *Rana* phylogeny (Hillis and Wilcox 2005; Frost *et al.* 2006; Dubois 2007a), the taxonomy of this group is currently in a state of flux, with four major nomenclatural proposals having been put forward in the past 15 years (Dubois 1992, 2007a; Hillis and Wilcox 2005; Frost *et al.*

2006). Given the unresolved disagreements among systematists regarding potential changes to *Rana* taxonomy (e.g. Dubois 2007a,b; Hillis 2007), I have chosen to follow past usage and employ the traditional genus name *Rana* for all of the American species investigated in this paper. However, newly proposed clade names are referenced where appropriate.

One of the major unresolved questions regarding *Rana* phylogeny is the phylogenetic position of *R. sylvatica* (Fig. 1). Various authors have grouped this species with either (1) the eastern American + neotropical *Rana* (= *Novirana* of Hillis and Wilcox 2005; *Lithobates* of Frost *et al.* 2006 and Dubois 2007a), or (2) the western American *Rana* + Eurasian *R. temporaria* group (= *Laurasiarana* of Hillis and Wilcox 2005; *Rana* of Frost *et al.* 2006 and Dubois 2007a). The addition of extensive molecular data has failed to resolve the phylogenetic position of *R. sylvatica*. For example, Hillis and Wilcox (2005) suggested that *R. sylvatica* is the sister taxon to the traditional *R. catesbeiana* group (= *Aquarana*;

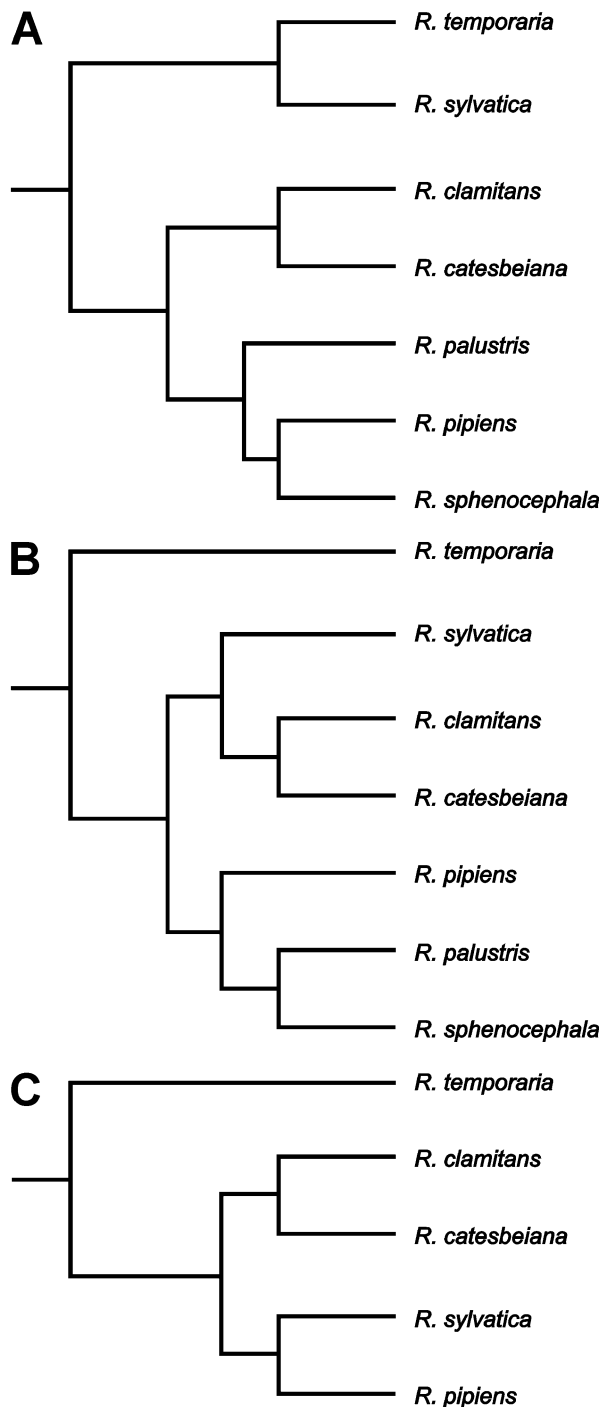


Fig. 1—Phylogenetic hypotheses for species of *Rana* examined in this study. Note the variable placement of *Rana sylvatica*. —**A**. Cladogram based on allozyme, immunological, morphological, and rDNA data (Hillis *et al.* 1983; Hillis and Davis 1986); —**B**. Cladogram based on mitochondrial DNA data (Hillis and Wilcox 2005); —**C**. Cladogram based on morphology, mitochondrial DNA, nuclear DNA, and ribosomal RNA data (Frost *et al.* 2006). Data from *Rana palustris* and *Rana sphenoccephala* were not included in the Frost *et al.* (2006) study.

Fig. 1B), whereas Frost *et al.* (2006) suggested a closer relationship between *R. sylvatica* and the traditional *Pantherana-Sierrana-Lithobates-Tryphlopsis* clade (represented by *R. pipiens* in Fig. 1C). The results of both of these studies support the grouping of *R. sylvatica* with the eastern American + Neotropical *Rana*, although the specific position of *R. sylvatica* within this larger clade was weakly corroborated and remains uncertain. Uncertainty regarding the phylogenetic position of *Rana sylvatica* has complicated attempts to revise *Rana* taxonomy, and resolving the placement of this species would greatly help to solidify any newly accepted taxonomy for this group.

Despite their relative ease of collection and common usage in scientific studies, descriptive/functional studies of larval musculoskeletal anatomy among species of *Rana* have focused primarily on only a few focal taxa (e.g. *R. temporaria*: Parker 1871; Gaupp 1893; de Beer 1937; Pusey 1938; de Jongh 1968; Plasota 1974; *R. catesbeiana*: Gradwell 1968, 1972a,b; Larson and Reilly 2003). Larvae of North American *Rana* are conservative in external morphology, particularly among leopard frogs of the traditional *R. pipiens* species group (Wassersug 1976; Hillis and Wilcox 2005). Despite the strong morphological similarity among species, studies have identified subtle morphometric differences in external larval anatomy (Korky 1978; Hillis 1982; Jennings and Scott 1993). Furthermore, Larson (2005) demonstrated clear morphometric differences in chondrocranial shape among *Rana* larvae, with patterns of similarity broadly matching expectations based on hypothesized phylogenetic relationships among species. However, the latter study focused only on quantitative variation in chondrocranial shape, and a detailed comparative description of larval chondrocranial morphology was not provided.

The availability of phylogenetic hypotheses of relationships among species of *Rana* (Fig. 1) make this group ideally suited to a comparative analysis of chondrocranial morphology (Hillis *et al.* 1983; Hillis and Davis 1986; Hillis and Wilcox 2005; Frost *et al.* 2006). Furthermore, although qualitative data on chondrocranial morphology and/or development are available for several species of *Rana* (e.g. *R. temporaria*: Parker 1871; Gaupp 1893; de Beer 1937; Pusey 1938; de Jongh 1968; Plasota 1974; *R. clamitans*: Parker 1881; *R. palustris*: Stone 1929; *R. pipiens*: Parker 1881; Kemp and Hoyt 1969; Alley 1989; *R. sylvatica*: Larson 2002), available descriptions vary considerably in detail, and all of these descriptions predate the most recently published phylogenetic hypotheses for *Rana* (Hillis and Wilcox 2005; Frost *et al.* 2006). As a result, a detailed comparison of qualitative variation in chondrocranial anatomy among larval *Rana* in a phylogenetic context is not available. Thus, the goals of this study are to: (1) provide a detailed comparative description of chondrocranial morphology for six species of North American *Rana*; and (2) interpret variation in chondrocranial morphology among larval *Rana* within a phylogenetic context (using *Rana temporaria* as an outgroup).

Materials and Methods

Material examined

Chondrocranial descriptions are based on 206 tadpoles representing six species of North American *Rana* (Appendix 1). Species included are *R. catesbeiana*, *R. clamitans*, *R. palustris*, *R. pipiens*, *R. sphenoccephala* and *R. sylvatica*. To control for ontogenetic variation, the specimens examined were chosen to approximate 'terminal' larval chondrocranial morphology for each species; this was done by selecting a threshold snout–vent length above which specimens for each species could be examined (see Larson 2005 for rationale and further details). Threshold snout–vent length and sample sizes for each species are: *R. catesbeiana* (24 mm, $n = 28$), *R. clamitans* (20 mm, $n = 38$), *R. palustris* (16 mm, $n = 34$), *R. pipiens* (18 mm, $n = 38$), *R. sphenoccephala* (15 mm, $n = 33$) and *R. sylvatica* (11 mm, $n = 35$). Most specimens represent Gosner stages 33–39, although some large specimens at earlier stages are also included. To further account for potential intraspecific variation, samples were examined from multiple geographical localities for most species (Appendix 1). Eight specimens of *R. temporaria* (snout–vent length range: 11.7–14.1 mm) from Erfurt, Germany were also examined as an outgroup.

Methods

The larvae examined represent both field-collected and laboratory-reared individuals. All larvae were killed with tricaine methanesulphonate (MS-222, Argent Chemical Laboratories, Redmond, WA) and preserved in formalin. Tadpoles were staged according to the table described by Gosner (1960) for staging anuran larvae, and callipers were used to record both total length and snout–vent length (to the nearest 0.01 mm) for each individual. All larvae were subsequently cleared and double-stained for bone and cartilage following a modification of the technique of Dingerkus and Uhler (1977). Chondrocranial terminology follows Cannatella (1999). Chondrocranial and hyobranchial images of *Rana* larvae were taken digitally with a Panasonic WV-BL200 BW CCD video camera mounted on a Nikon SMZ-U Zoom 1 : 10 dissecting microscope; images were captured and imported into a computer by a DAZZLE DVC framegrabber (DAZZLE MULTIMEDIA). Illustrations were made by digitally tracing images in CORELDRAW 9 (Corel Corporation 1999).

Results

Chondrocranial and hyobranchial morphology are qualitatively similar among the species examined here (Figs 2 and 3). As such, the following chondrocranial description applies to all species of *Rana* examined; individual species differences are noted where appropriate. Unless otherwise noted, abbreviations are those used in Fig. 4.

Upper jaws and ethmoid region

The paired elements of the larval upper jaw are fused to form a single continuous suprarostrals cartilage (sr; Figs 4A and 5A) in *Rana*. The central suprarostrals corpora (sc; Fig. 5A), located medially, extend further dorsally than the lateral alae (sa; Fig. 5A), resulting in a sloping dorsal suprarostrals margin. The corpora are wide strips of cartilage that are extensively fused ventromedially, along approximately one-half to three-quarters of their length. Their dorsal divergence typically forms a shallow U-shape; the region of fusion between the corpora is frequently pierced by additional small holes (e.g. Fig. 5A). The plate-like alae, located laterally, are extensively fused to the corpora both dorsally and ventrally, with a variably sized hole separating these connections (Fig. 5A). A well-developed posterior dorsal process (pdp; Fig. 5A) extends from the posterodorsal margin of each ala. The trabecular horns articulate with the dorsal margins of the alae.

The trabecular horns (th; Fig. 4A,B) in *Rana* diverge anteriorly from the ethmoid plate and are long, slender, and widen proximally to distally. The divergence between the trabecular horns widens only slightly anteriorly, resulting in a deep, narrow, U-shaped separation (Figs 2 and 4A). Anterolaterally, the trabecular horns flex ventrally to articulate with the suprarostrals (Fig. 4B). A distinct lateral trabecular process extends from the lateral margin of each trabecular horn as a rounded or triangular bump in most specimens of *R. clamitans* and several specimens of *R. catesbeiana* (Arrow 1 in Fig. 2D,E).

Braincase

When fully developed, the floor of the braincase in *Rana* larvae is formed by the planum intertrabeculare. The planum intertrabeculare is bordered anteriorly by the planum trabecularum anticum, laterally by the trabecular cartilages (tc; Fig. 4B), and posteriorly by the basal plate. Two sets of foramina perforate the floor of the braincase: the craniopalatine foramina (crf; Fig. 4A), and the primary carotid foramina (located posteriorly). The primary carotid foramina are typically obscured in dorsal view by the taenia tecti transversales (ttt; Fig. 4A); however, they can be seen in Fig. 1A and F. In most specimens examined, the frontoparietal fenestra is fully subdivided into a frontal fenestra and two parietal fenestrae (pf; Fig. 4A). This subdivision is achieved through medial growth of the taenia tecti transversales (ttt), and anterior growth of the taenia tectum medialis (ttm) from the tectum synoticum (ts).

The lateral walls of the braincase are formed dorsally by the orbital cartilages (orc; Fig. 4B) and ventrally by the trabecular cartilages (tc). The orbital cartilages are poorly developed in *Rana*, typically only forming anteriorly, dorsal to the anterior quadratocranial commissure, and posteriorly in the region dorsal to the pila antotica. In most specimens,

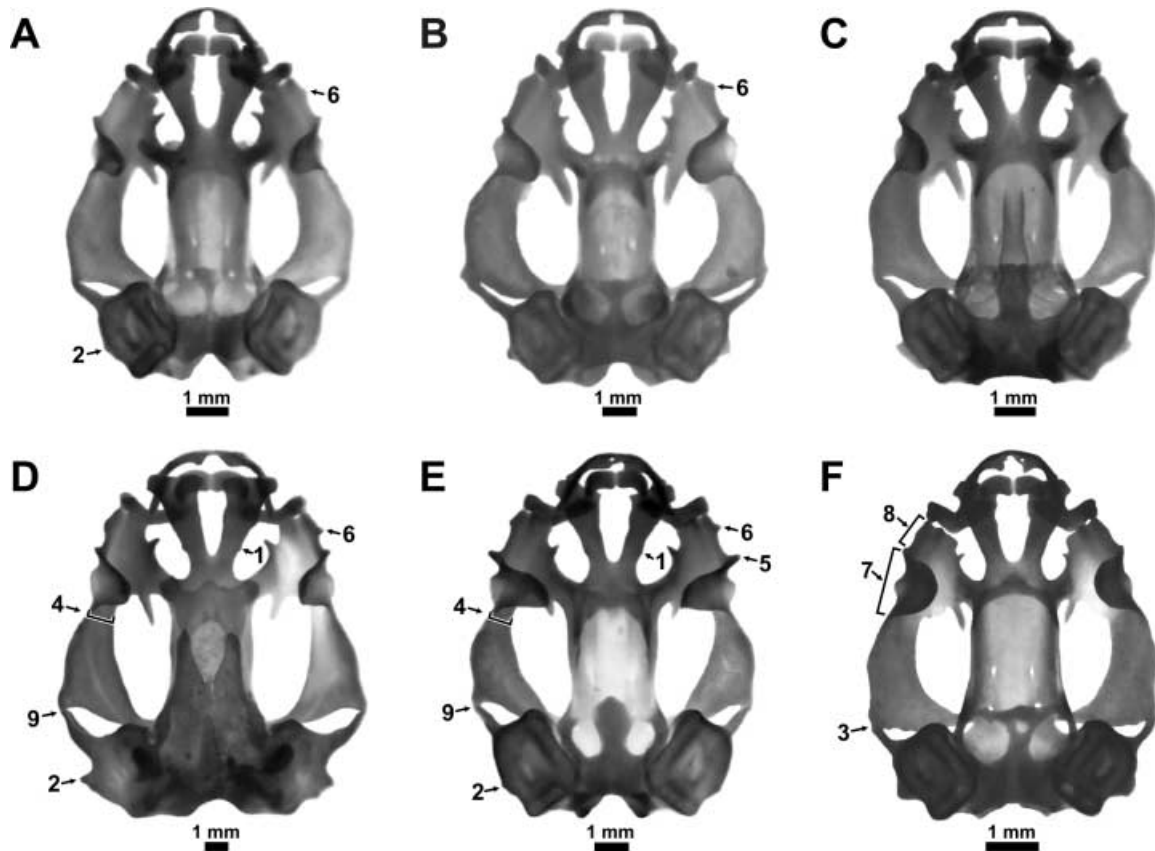


Fig. 2—Representative dorsal views of *Rana* chondrocrania. —A. *Rana palustris*, Stage 36, snout–vent length (SVL) = 17.5 mm; —B. *R. pipiens*, Stage 37, SVL = 23.3 mm; —C. *R. sphenoccephala*, Stage 38, SVL = 19.3 mm; —D. *R. catesbeiana*, Stage 37, SVL = 33.9 mm; —E. *R. clamitans*, Stage 38, SVL = 23.3 mm; —F. *R. sylvatica*, Stage 37, SVL = 14.3 mm. Numbered arrows and brackets indicate specific characters discussed in the text.

chondrification in the region of the pila metoptica is sufficient to fully enclose the oculomotor foramen (ocf; Fig. 4B). The optic foramen is typically only visible as a dorsal indentation of the trabecular cartilages, just anterior to the oculomotor foramen. The posterodorsal connection of the orbital cartilage to the medial margin of the otic capsule via the taenia tecti marginales (ttg) forms the dorsal margin of the prootic foramen (prf), an elongate opening located rostral to the anterior edge of the otic capsule. In well-developed specimens, the taenia tecti marginales (ttg; Fig. 4B) form a complete strip of cartilage along the dorsolateral margin of the braincase, connecting the anterior and posterior chondrified regions. Combined with poor chondrification of the orbital cartilages, this gives the appearance of a large medial opening in each side of the braincase (see Fig. 4B).

Otooccipital region

The otic capsules (oc; Fig. 4A) are large and ovoid in shape. In dorsal view, they bear a laterally projecting, variably sized larval crista parotica (lcp). The presence of a posterolateral

process of the larval crista parotica is intraspecifically variable. When present, it varies in size among specimens from being large and triangular (Arrow 2 in *R. catesbeiana*, Fig. 2D) to a small bump (Arrow 2 in Fig. 2A,E). The anterolateral process of the larval crista parotica extends from the lateral margin of the otic capsule and fuses to the posterolateral margin of the palatoquadrate; thus, a larval otic process (lop; Fig. 4A,B) is present in these species. In most species (Fig. 2A–E), the larval otic process is elongate and extends anterolaterally and ventrally to fuse with the palatoquadrate; this fusion typically occurs at approximately the level of the anterior margin of the otic capsule in *R. palustris*, *R. pipiens* and *R. sphenoccephala* (Fig. 2A–C), and slightly further anteriorly in *R. catesbeiana* and *R. clamitans* (Fig. 2D,E). In *R. sylvatica* (Arrow 3 in Fig. 2F), the larval otic process extends almost directly ventrolaterally to attach to the palatoquadrate at a level posterior to the anterior margin of the otic capsule. An additional connection between the otic capsule and palatoquadrate was observed on one side of the body in two specimens of *R. pipiens*. In these specimens, a rod of cartilage extends from the floor of the otic capsule, just

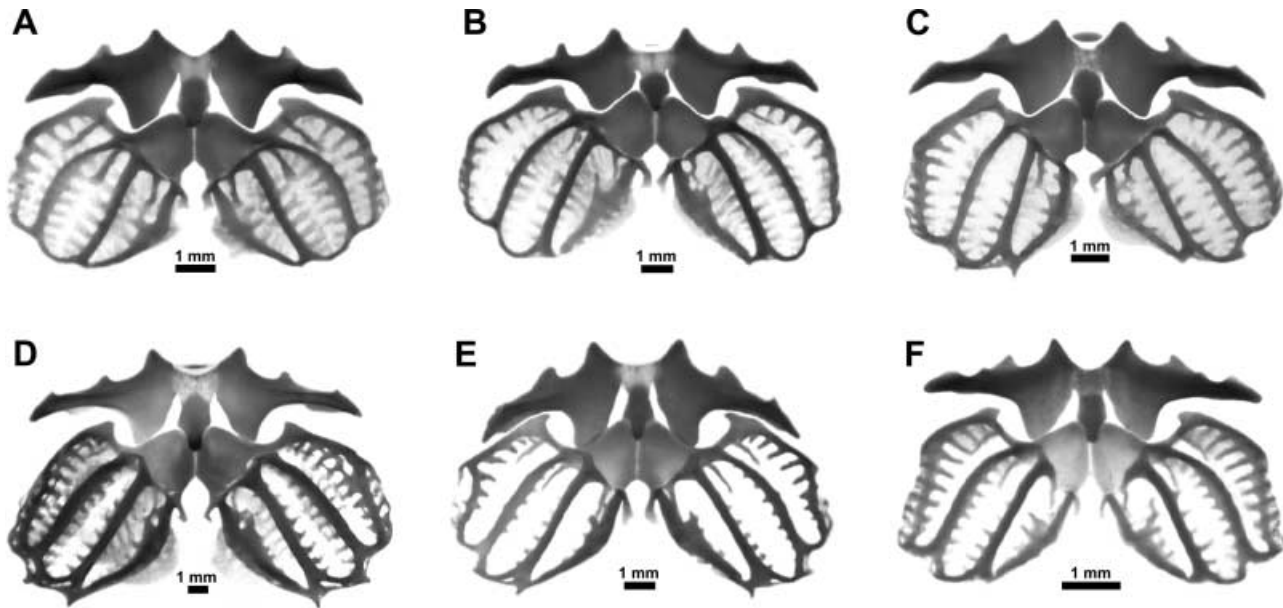


Fig. 3—Representative ventral views of the hyobranchial apparatus in *Rana*. —**A.** *Rana palustris*, Stage 36, snout–vent length (SVL) = 17.5 mm; —**B.** *R. pipiens*, Stage 37, SVL = 23.3 mm; —**C.** *R. sphenocephala*, Stage 38, SVL = 19.3 mm; —**D.** *R. catesbeiana*, Stage 37, SVL = 33.9 mm; —**E.** *R. clamitans*, Stage 38, SVL = 23.3 mm; —**F.** *R. sylvatica*, Stage 39, SVL = 12.1 mm.

below the foramen ovale, and attaches to the posteromedial margin of the palatoquadrate. This probably corresponds to a palatobasal connection as described by other authors (Haas and Richards 1998; Haas 2003). A fingerlike process extending from the same region of the palatoquadrate (but not fusing with the otic capsule) was observed on one side of the body in a single specimen of *R. sphenocephala*.

The otic capsules in *Rana* are interconnected medially by a wide tectum synoticum (ts), which results in the posterior margins of the parietal fenestrae being located at or just anterior to the level of the midpoint of the otic capsules (Figs 2 and 4A). Each otic capsule is connected to the basal plate via the occipital arch (oa; Fig. 4B); the latter structure forms the ventral and medial margins of the jugular foramen. A large fenestra ovalis (fov; Fig. 4B) perforates the ventrolateral wall of the otic capsule, just beneath the larval crista parotica. The inferior perilymphatic foramen can be observed piercing the otic capsule ventromedially.

Palatoquadrate

The palatoquadrate of *Rana* is long, wide and orientated approximately parallel to the main body axis. In *R. sylvatica*, the palatoquadrate extends farther posteriorly and is broader at its posterior extent (Fig. 2F). Also, the posterior margin of the palatoquadrate in *R. sylvatica* is approximately perpendicular to the main body axis, whereas in all other species examined it angles anteriorly from its medial to lateral margin. In *R. catesbeiana* and *R. clamitans* (Fig. 2D,E), the

palatoquadrate is distinctly narrower than in other species in the region just posterior to the muscular process (Bracket 4 in Fig. 2F).

The palatoquadrate attaches to the braincase by two cartilaginous connections: the ascending process (apr; Fig. 4A) and the anterior quadratocranial commissure (aqc). The ascending process is a narrow, rod-like, cartilage that connects the posteromedial margin of the palatoquadrate to the region of the pila antotica, just behind the posterior margin of the oculomotor foramen.

The anterior quadratocranial commissure is a wide cartilaginous strut that extends between the anteromedial margin of the palatoquadrate and the floor of the neurocranium. The anterior margin of the anterior quadratocranial commissure bears a triangular quadratoethmoid process (qp; Fig. 4A); a fingerlike pseudopterygoid process (pp) extends from the posterior margin. Occasionally, a secondary projection, the processus medialis (pm; Haas 1999), can be seen extending from the medial margin of the palatoquadrate adjacent to the pseudopterygoid process (e.g. Fig. 4A). A quadrato-orbital commissure connecting the muscular process (mp) of the palatoquadrate to the anterior quadratocranial commissure is absent in all *Rana* examined. In the late-stage specimens examined here, the nasal tectum (nt) and nasal septum (ns) can typically be seen in the ethmoid region, dorsomedial to the anterior quadratocranial commissure (e.g. Fig. 4A,B).

The muscular process (mp; Fig. 4A,B) extends dorsomedially from the lateral margin of the palatoquadrate, almost to the level of the dorsal surface of the braincase. It is broad,

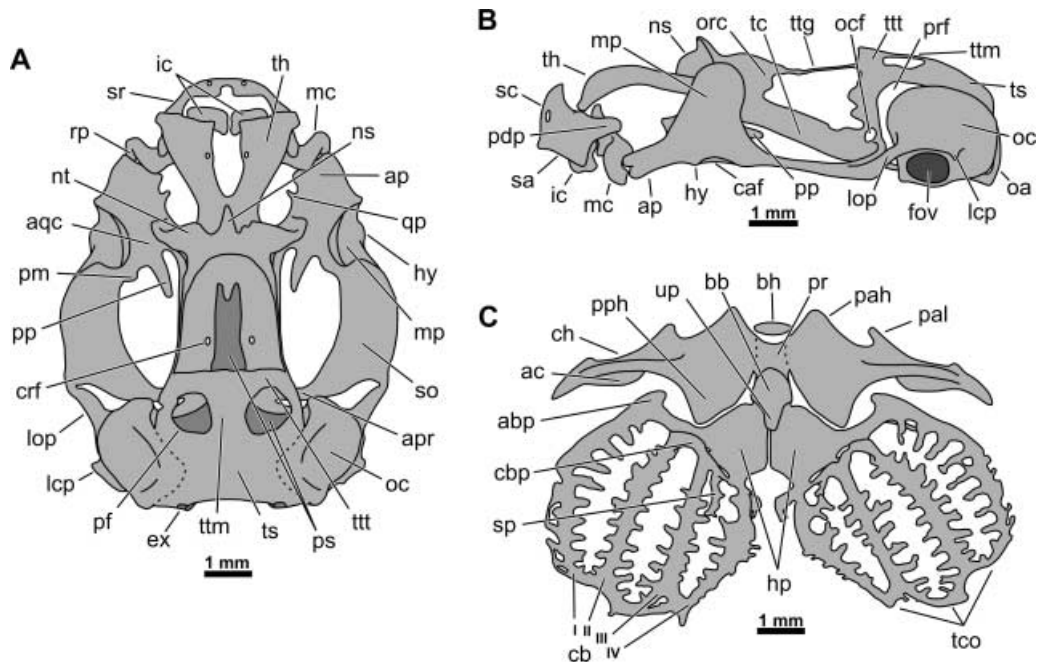


Fig. 4—Chondrocranium and hyobranchial apparatus of a representative *Rana* larva (*Rana sphenoccephala*, Stage 38, snout-vent length = 19.3 mm). —**A**. Dorsal view of chondrocranium; —**B**. Lateral view of chondrocranium; —**C**. Ventral view of the hyobranchial apparatus. Frontoparietal bones were present slightly anterior to the parietal foramina, but were small and faintly stained and are thus not illustrated here. abp – anterior branchial process, ac – articular condyle, ap – articular process, apr – ascending process, aqc – anterior quadrato cranial commissure, bb – basibranchial, bh – basihyal, caf – ceratohyal articular facet, cb I–IV – ceratobranchial cartilages I–IV, ch – ceratohyal, cbp – closed branchial process, crf – craniopalatine foramen, ex – exoccipital, fov – fenestra ovalis, hp – hypobranchial plates, hy – hyoquadrate process, ic – infrarostral cartilages, lcp – larval crista parotica, lop – larval otic process, mc – Meckel’s cartilage, mp – muscular process, ns – nasal septum, nt – nasal tectum, oa – occipital arch, oc – otic capsule, ocf – oculomotor foramen, orc – orbital cartilage, pah – processus anterior hyalis, pal – processus anterolateralis hyalis, pdp – posterior dorsal process, pf – parietal foramen, pm – medial process of palatoquadrate, pp – pseudopterygoid process, pph – processus posterior hyalis, pr – pars reuniens, prf – prootic foramen, ps – parasphenoid, qp – quadratoethmoid process, rp – retroarticular process of Meckel’s cartilage, sa – suprarostal ala, sc – suprarostal corpus, so – subocular bar of palatoquadrate, sp – spicule, sr – suprarostal cartilage, tc – trabecular cartilage, tco – terminal commissures, th – trabecular horns, ts – tectum synoticum, ttg – taenia tecti marginales, ttm – taenia tecti medialis, ttt – taenia tecti transversales, up – urobranchial process.

flat, and dorsally rounded; it is wider from anterior to posterior in *R. sylvatica* than in other species (Bracket 7 in Fig. 2F). The anterior margin of the muscular process typically curls laterally, such that it extends beyond the lateral margin of the palatoquadrate in dorsal view; this curvature tends to be exaggerated in *R. clamitans* (Arrow 5 in Fig. 2E). Ventral to the muscular process, the hyoquadrate process (hy; Fig. 4B) forms the anterior margin of the ceratohyal articular facet (caf), which serves as the point of articulation of the ceratohyal to the palatoquadrate. The articular process of the palatoquadrate, which serves as the point of articulation for the lower jaws, is shorter and wider in *R. sylvatica* when compared to the other species (Bracket 8 in Fig. 2F). The lateral margin of the articular process often bears a variably developed, triangular, secondary process (Arrow 6 in Fig. 2A,B,D,E).

Lower jaws

Meckel’s cartilage (mc; Figs 4A and 5B) is stout, sigmoid shaped, and bears a lateral retroarticular process (rp) that curls underneath the articular process of the palatoquadrate. At its medial tip, Meckel’s cartilage bears dorsal and ventral processes that form a facet for the articulation of the infrarostral cartilages. The infrarostral cartilages (ic; Figs 4A and 5B), which support the keratinous lower jaw sheath, are wedge shaped and connect to each other medially.

Hyobranchial apparatus

Hyobranchial morphology is similar among species examined here (Fig. 3). The ceratohyal cartilages (ch; Fig. 4C) are thick, transversely orientated, and bear a dorsolateral articular

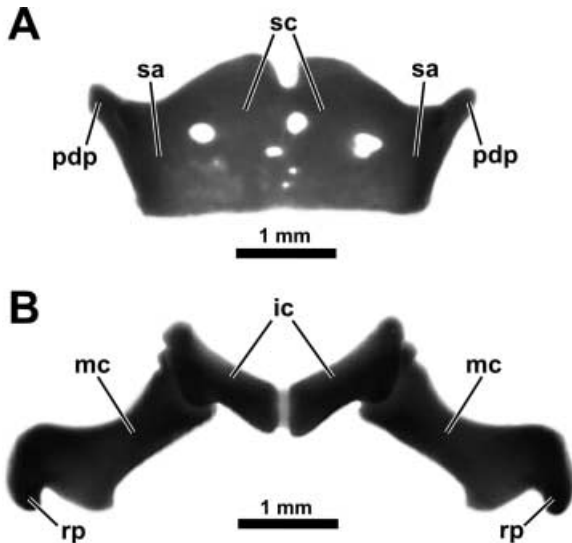


Fig. 5—Upper and lower jaws of *Rana clamitans* (Stage 38, snout–vent length = 23.4 mm). —**A**. Anterior view of upper jaw cartilage; —**B**. ventral view of lower jaw cartilages. ic – infra-rostral cartilage; pdp – posterior dorsal process; rp – retroarticular process; sa – supra-rostral alae; sc – supra-rostral corpora.

condyle (ac) that articulates with the palatoquadrate at the ceratohyal articular facet. Three other processes are found on each ceratohyal: a large, triangular processus anterior hyalis (pah) located anteromedially, a more lateral, attenuate processus anterolateralis hyalis (pal), and a large, triangular processus posterior hyalis (pph) extending from the postero-medial margin (Fig. 4C). Medially, the ceratohyals are interconnected by the pars reuniens (pr), a flexible cartilage that allows for bending of the hyobranchial apparatus during buccal pumping. The presence of a basihyal (bh; Fig. 4C), located anterior to the pars reuniens, was intraspecifically variable (Fig. 3); however, it was found in at least some specimens of every species. When present, the basihyal varied considerably in size and shape (e.g. compare Fig. 3C,D). The pars reuniens connects posteriorly to the basibranchial (bb), which bears a stout or fingerlike urobranchial process (up) extending posteriorly from its ventral surface. The basibranchial connects posteriorly to the hypobranchial plates (hp).

The hypobranchial plates are wide, flat cartilages that serve as the point of attachment for the ceratobranchial cartilages (cb I–IV; Fig. 4C). There is no distinct medial fusion between these plates (Fig. 3), although light chondrification appears posteriorly in some specimens. The branchial baskets consist of four ceratobranchials that are distally continuous via terminal commissures (tco). Proximally, Ceratobranchial I fuses widely to the hypobranchial plate and bears a hook-like anterior branchial process (abp) on its anterior margin. Ceratobranchials II and III are connected proximally by a closed branchial process (cbp), although the

connections of these ceratobranchials to the hypobranchial plates are somewhat variable among specimens. Ceratobranchial II is either fused narrowly to the hypobranchial plate or does not exhibit a cartilaginous connection. Ceratobranchial III typically has an indirect fusion to the hypobranchial plate. This is achieved via a short rod of cartilage that fuses proximally to Ceratobranchial IV, with the latter being fused directly to the posterior portion of the hypobranchial plate (e.g. Fig. 4C). Occasionally, however, Ceratobranchials III and IV appear to share a common fusion to the hypobranchial plate. All ceratobranchials bear a dorsally projecting spiculum (sp.).

Discussion

Although previous research indicates that larval chondrocranial shape is morphometrically distinguishable among species of *Rana* (Larson 2005), chondrocranial and hyobranchial morphology are qualitatively similar among the larvae examined here (Figs 2 and 3), and discrete morphological differences were difficult to identify. Despite this, a few variable characters were identified that provide support for clades within the genus *Rana*, and other characters were identified that seem to further complicate hypotheses regarding the phylogenetic position of *R. sylvatica*.

Rana sylvatica can be qualitatively differentiated from all other species on the basis of the presence of (1) a broader posterior palatoquadrate, resulting in a more posterior level of attachment of the larval otic process to the palatoquadrate (Arrow 3 in Fig. 2F), (2) a wider muscular process of the palatoquadrate (Bracket 7 in Fig. 2F), and (3) a short palatoquadrate articular process (Bracket 8 in Fig. 2F). These distinct conditions are supported by past morphometric analysis (Larson 2005), and are similar to those found in *R. temporaria* (de Beer 1937; Pusey 1938; de Jongh 1968). However, in the absence of chondrocranial data on additional species of Eurasian or western North American *Rana*, it is difficult to come to a firm conclusion regarding the generality or phylogenetic importance of these findings. Despite this, it is clear that chondrocranial anatomy in *R. sylvatica* is distinct from that seen in other eastern North American *Rana*. Given that these morphologically distinct structures are all parts of the larval feeding apparatus, it is possible that the unique anatomy of *R. sylvatica* could relate to behavioural or ecological differences with other species (e.g. habitat, diet, activity level, etc.). Assessment of the relative role of phylogeny versus ecology in the shaping of chondrocranial anatomy awaits further study.

Additional chondrocranial characters were identified that may represent synapomorphies for the traditional *R. catesbeiana* group (= *Aquarana*). These include the following: (1) the palatoquadrate is markedly narrower in *R. catesbeiana* and *R. clamitans* in the region just posterior to the anterior quadratocranial commissure (Bracket 4 in Fig. 2D,E), and (2) the connection between the larval otic process and the

palatoquadrate is located farther anteriorly in these species (Arrow 9 in Fig. 2D,E). *Rana catesbeiana* and *R. clamitans* were also the only species in which a distinct lateral trabecular process was observed in at least some specimens (Arrow 1 in Fig. 2D,E), but this character was only variably present in these species and its strength as a diagnostic character is thus questionable.

In one of the few existing comparative analyses of chondrocranial anatomy among *Rana* larvae, Parker (1881) compared the chondrocranium of *R. clamitans* to that of *R. pipiens* and noted that the chondrocranium of *R. pipiens* is ‘altogether rounder, less angular, and free from the projecting snags’ when compared to that of *R. clamitans*. Whereas many of the differences observed by Parker (1881) between these two species do not hold up to further analysis with larger sample sizes and modern staining and morphometric techniques, this simple observation effectively describes the distinctive appearance of the chondrocrania of the clades that these two species represent. Unfortunately, such anecdotal observations are difficult to encapsulate as phylogenetic characters, and this is partly why effective methods for the integration of morphometric shape data into phylogenetic analyses are so badly needed. The chondrocrania of the major groupings of species examined here are qualitatively distinct; however, most of the differences are subtle and are difficult to describe without the aid of morphometric analysis. At the same time, morphometric analysis is only as good as the measurements/landmarks chosen for examination. Studies that employ both qualitative and quantitative approaches are ideal because morphometric analysis (e.g. Larson 2005) can highlight differences that might not be immediately apparent upon qualitative observation (e.g. character indicated by bracket 8 in Fig. 2F), whereas qualitative observation allows for detailed description and identification of differences that might not be picked up by the measurements chosen for analysis in morphometric studies (e.g. character 4 indicated in Fig. 2D,E).

A few larval characters that have been analysed in previous studies of anuran phylogeny were found to be intraspecifically variable among the specimens of *Rana* examined here (Larson and de Sá 1998; Maglia *et al.* 2001; Haas 2003; Púgner *et al.* 2003). These include the presence of a posterolateral process of the larval crista parotica (e.g. Arrow 2 in Fig. 2D), and the presence of a basihyal cartilage (= copula I) located anterior to the pars reunions (Fig. 3C). The basihyal, for example, was reported as present in the seven ranids examined by Haas (2003), and was present in at least some, but not all specimens of all six North American species examined here (at times, it was not visible in whole mount specimens as late as Stage 39). This character was also found to be intraspecifically variable in dendrobatids (Haas 1995), and its state may be only definitively determinable through histological examination (Haas 2003). These results indicate that examination of small sample sizes of whole-mount specimens could lead to potentially misleading conclusions

about the presence or absence of certain structures, complicating analyses of their phylogenetic distribution.

Whereas the number of variable characters identified in the present study was small, these results combined with those presented by Larson (2005) do suggest that larval chondrocranial anatomy is phylogenetically informative. For example, pending further taxon sampling, characters supporting supraspecific clades (e.g. the *R. catesbeiana* group/*Aquarana*) were identified. Unfortunately, the addition of larval chondrocranial data does little to resolve the phylogenetic position of *R. sylvatica*; in fact characters shared with *R. temporaria* would seem to support older phylogenies that group *R. sylvatica* with this Eurasian species (Fig. 1A; Farris *et al.* 1979, 1982; Hillis and Davis 1986). However, this relationship is not supported by recent molecular data (Fig. 1B,C; Hillis and Wilcox 2005; Frost *et al.* 2006). Thus, *R. sylvatica* continues to be enigmatic, and a more comprehensive analysis of the phylogenetic position of this species within the genus is needed, particularly because this lack of resolution represents one of the major complicating factors regarding any potential taxonomic revision of this group of frogs.

Acknowledgements

I am grateful to Alex Haas for loaning the specimens of *Rana temporaria* taxa examined in this study. Thanks are also due to Robert Murphy of the Royal Ontario Museum and Ron Heyer of the Smithsonian Institution for the loan of specimens. Rick Essner, Brian Knapp, Joe Mitchell, Gerry Svendsen, Gary Radice and Steve Reilly provided field-caught specimens or allowed access to their land for field collection. The Wayne National Forest and Ohio Department of Natural Resources provided permits allowing collection of many of the specimens examined here. I am grateful to Chris Swart for preparing a number of the specimens and I would like to thank Larry Witmer, Bob Carr and Audrone Biknevičius for providing helpful comments on earlier drafts of the manuscript. Steve Reilly provided many of the resources necessary for the completion of this work and was an incredibly helpful source of advice throughout. This research was partially funded by a Grant in Aid of Research from Sigma Xi, and by research funds from the Biology Department at Saint Anselm College.

References

- Alley, K. E. 1989. Myofiber turnover is used to retrofit frog jaw muscles during metamorphosis. – *American Journal of Anatomy* 184: 1–12.
- de Beer, G. R. 1937. *The Development of the Vertebrate Skull*. Oxford University Press, Oxford.
- Cannatella, D. 1999. Architecture: cranial and axial musculoskeleton. In McDiarmid, R. W. and Altig, R. (Eds): *Tadpoles: The Biology of Anuran Larvae*, pp. 52–91. University of Chicago Press, Chicago.
- Case, S. M. 1978. Biochemical systematics of the genus *Rana* native to western North America. – *Systematic Zoology* 27: 299–311.

- Chantell, C. J. 1970. Upper Pliocene frogs from Idaho. – *Copeia* 1970: 654–664.
- Dingerkus, G. and Uhler, L. D. 1977. Enzyme clearing of alcian blue stained whole small vertebrates for demonstration of cartilage. – *Stain Technology* 52: 229–232.
- Dubois, A. 1992. Notes sur la classification des Ranidae (Amphibiens Anoures). – *Bulletin Mensuel de la Société Linnéenne de Lyon* 61: 305–352.
- Dubois, A. 2007a. Naming taxa from cladograms: a cautionary tale. – *Molecular Phylogenetics and Evolution* 42: 317–330.
- Dubois, A. 2007b. Naming taxa from cladograms: some confusions, misleading statements, and necessary clarifications. – *Cladistics* 23: 1–13.
- Farris, J. S., Kluge, A. G. and Micklevech, M. F. 1979. Paraphyly of the *Rana boylei* group. – *Systematic Zoology* 28: 627–634.
- Farris, J. S., Kluge, A. G. and Micklevech, M. F. 1982. Immunological distance and the phylogenetic relationships of the *Rana boylei* species group. – *Systematic Zoology* 31: 479–491.
- Frost, D. R., Grant, T., Faivovich, J., Bain, R. H., Haas, A., Haddad, C. F., de Sá, R. O., Channing, A., Wilkinson, M., Donnellan, S. C., Raxworthy, C. J., Campbell, J. A., Blotto, B. L., Moler, P., Drewes, R. C., Nussbaum, R. A., Lynch, J. D., Green, D. M. and Wheeler, W. C. 2006. The amphibian tree of life. – *Bulletin of the American Museum of Natural History, New York* 297: 1–291.
- Gaupp, E. 1893. Beiträge zur Morphologie des Schädels. I: Primordial-Cranium und Kieferbogen von *Rana fusca*. – *Morphologische Arbeiten* 2: 275–481.
- Gosner, K. L. 1960. A simplified table for staging anuran embryos and larvae with notes on identification. – *Herpetologica* 16: 183–190.
- Gradwell, N. 1968. The jaw and hyoidean mechanism of the bullfrog tadpole during aqueous ventilation. – *Canadian Journal of Zoology* 46: 1041–1052.
- Gradwell, N. 1972a. Gill irrigation in *Rana catesbeiana*. Part I. On the anatomical basis. – *Canadian Journal of Zoology* 50: 481–499.
- Gradwell, N. 1972b. Gill irrigation in *Rana catesbeiana*. Part II. On the musculoskeletal mechanism. – *Canadian Journal of Zoology* 50: 501–521.
- Haas, A. 1995. Cranial features of dendrobatid larvae (Amphibia: Anura: Dendrobatidae). – *Journal of Morphology* 224: 241–264.
- Haas, A. 1999. Larval and metamorphic skeletal development in the fast developing frog *Pyxicephalus adspersus* (Anura, Ranidae). – *Zoomorphology* 119: 23–35.
- Haas, A. 2003. Phylogeny of frogs as inferred from primarily larval characters (Amphibia: Anura). – *Cladistics* 19: 23–89.
- Haas, A. and Richards, S. J. 1998. Correlations of cranial morphology, ecology, and evolution in Australian suctorial tadpoles of the genera *Litoria* and *Nyctimystes* (Amphibia: Anura: Hylidae: Pelodyadinae). – *Journal of Morphology* 238: 109–141.
- Hillis, D. M. 1982. Morphological differentiation and adaptation of the larvae of *Rana berlandieri* and *Rana sphenoccephala* (*Rana pipiens* complex) in sympatry. – *Copeia* 1982: 168–174.
- Hillis, D. M. 1988. Systematics of the *Rana pipiens* complex: puzzle and paradigm. – *Annual Review of Ecology and Systematics* 19: 39–63.
- Hillis, D. M. 2007. Constraints in naming parts of the Tree of Life. – *Molecular Phylogenetics and Evolution* 42: 331–338.
- Hillis, D. M. and Davis, S. K. 1986. Evolution of ribosomal DNA: fifty million years of recorded history in the frog genus *Rana*. – *Evolution* 40: 1275–1288.
- Hillis, D. M. and de Sá, R. 1988. Phylogeny and taxonomy of the *Rana palmipes* group (Salientia: Ranidae). – *Herpetological Monographs* 2: 1–26.
- Hillis, D. M. and Wilcox, T. P. 2005. Phylogeny of the New World true frogs (*Rana*). – *Molecular Phylogenetics and Evolution* 34: 299–314.
- Hillis, D. M., Frost, J. S. and Wright, D. A. 1983. Phylogeny and biogeography of the *Rana pipiens* complex: a biochemical evaluation. – *Systematic Zoology* 32: 132–143.
- Jennings, R. D. and Scott, N. J. Jr. 1993. Ecologically correlated morphological variation in tadpoles of the leopard frog, *Rana chiricahuensis*. – *Journal of Herpetology* 27: 285–293.
- de Jongh, H. J. 1968. Functional morphology of the jaw apparatus of larvae and metamorphosing *Rana temporaria* L. – *Netherlands Journal of Zoology* 18: 1–103.
- Kemp, N. E. and Hoyt, J. A. 1969. Sequence of ossification in the skeleton of growing and metamorphosing tadpoles of *Rana pipiens*. – *Journal of Morphology* 129: 415–444.
- Korky, J. K. 1978. Differentiation of the larvae of members of the *Rana pipiens* complex in Nebraska. – *Copeia* 1978: 455–459.
- Larson, P. M. 2002. Chondrocranial development in larval *Rana sylvatica* (Anura: Ranidae): a morphometric analysis of cranial allometry and ontogenetic shape change. – *Journal of Morphology* 252: 131–144.
- Larson, P. M. 2005. Ontogeny, phylogeny, and morphology in anuran larvae: a morphometric analysis of cranial development and evolution in *Rana* larvae (Anura: Ranidae). – *Journal of Morphology* 264: 34–52.
- Larson, P. M. and de Sá, R. O. 1998. Chondrocranial morphology of *Leptodactylus* larvae (Leptodactylidae: Leptodactylinae): its utility in phylogenetic reconstruction. – *Journal of Morphology* 238: 287–305.
- Larson, P. M. and Reilly, S. M. 2003. Functional morphology of feeding and gill irrigation in the anuran tadpole: electromyography and muscle function in larval *Rana catesbeiana*. – *Journal of Morphology* 255: 202–214.
- Maglia, A. M., Pügener, L. A. and Trueb, L. 2001. Comparative development of anurans: using phylogeny to understand ontogeny. – *American Zoologist* 41: 538–551.
- Parker, W. K. 1871. On the structure and development of the skull of the common frog (*Rana temporaria* L.). – *Philosophical Transactions of the Royal Society of London* 161B: 137–211.
- Parker, W. K. 1881. On the structure and development of the skull in the Batrachia. Part III. – *Philosophical Transactions of the Royal Society of London* 172: 1–266.
- Plasota, K. 1974. The development of the chondrocranium (neurocranium and the mandibular and hyoid arches) in *Rana temporaria* L. & *Pelobates fuscus* (Laur.). – *Zoologica Poloniae* 24: 99–168.
- Post, T. J. and Uzzell, T. 1981. The relationships of *Rana sylvatica* and the monophyly of the *Rana boylei* group. – *Systematic Zoology* 30: 170–180.
- Pügener, L. A., Maglia, A. M. and Trueb, L. 2003. Revisiting the contribution of larval characters to an analysis of phylogenetic relationships of basal anurans. – *Zoological Journal of the Linnean Society* 139: 129–155.
- Pusey, H. K. 1938. Structural changes in the anuran mandibular arch during metamorphosis, with reference to *Rana temporaria*. – *Quarterly Journal of Microscopical Science* 80: 479–552.
- Stone, L. S. 1929. Experiments showing the role of migrating neural crest (mesectoderm) in the formation of the head skeleton and loose connective tissue in *Rana palustris*. – *Wilhelm Roux' Archiv für Entwicklungsmechanik der Organismen* 118: 40–77.
- Uzzell, T. and Post, T. J. 1986. *Rana temporaria* is not a member of the *Rana boylei* group. – *Systematic Zoology* 35: 414–421.
- Wallace, D. G., King, M. C. and Wilson, A. C. 1973. Albumin differences among ranid frogs: taxonomic and phylogenetic implications. – *Systematic Zoology* 22: 1–13.
- Wassersug, R. J. 1976. The identification of leopard frog tadpoles. – *Copeia* 1976: 413–414.

Appendix 1 List of specimens examined

Species	Collection locality/Source	Sample size	Gosner stages	SVL range
<i>Rana catesbeiana</i>	Long Lake, Harrison, ME	15	27–29, 31, 33–37, 39	24.5–35.1
	Nipissing, Ontario, Canada (ROM 21044*)	4	32–35	31.1–32.5
	Niagara, Ontario, Canada (ROM 12088*)	1	31	33.1
	Shade, Athens County, OH	6	31, 36–37, 39	28.3–36.8
	Lake Snowden, Athens County, OH	1	36	25.7
	Waterloo Wildlife Station, Athens County, OH	1	39	34.3
<i>Rana clamitans</i>	Ohio University Campus, Athens County, OH	21	30, 34–39	20.3–31.7
	Lake Hope, Vinton County, OH	3	31, 36	20.1–23.1
	Biehle, Perry County, MO	5	30, 35, 37, 39	20.1–27.1
	Jackson County, OH	3	31, 34, 38	20.2–23.4
	Minker's Run, Nelsonville, OH	3	36–38	24.9–25.7
	Waterloo Wildlife Station, Athens County, OH	1	37	26.7
<i>Rana palustris</i>	Virginia (USNM #299871†)	2	31, 34	21.7–22.6
	Charles D. Sullivan Co., Nashville, TN (Field Collected)	25	31, 33–39	16.0–22.5
<i>Rana pipiens</i>	Chapel Hill, Orange County, NC	9	31–32, 35, 37–39	17.7–23.7
	Nasco Science, Fort Atkinson, WI (1999)	29	31–39	18.3–29.1
<i>Rana sphenocephala</i>	Nasco Science, Fort Atkinson, WI (2001)	6	34–36	18.2–21.8
	Haldimand, Ontario, Canada (ROM 11945*)	3	32–34	18.1–18.4
<i>Rana sylvatica</i>	Charles D. Sullivan Co., Nashville, TN (Field Collected)	33	31–39	15.0–20.1
<i>Rana sylvatica</i>	Shade, Athens County, OH	26	31–39	11.1–14.3
	Fort A.P. Hill, Caroline County, VA	9	30–33, 35	11.9–14.2

ROM = Royal Ontario Museum; SVL = snout–vent length; USNM = United States National Museum, Smithsonian Institution.